Comparative study between the protective role of Rosmarinic acid (RA) and the effect of mesenchimal stem cells on ameliorating the toxic effect of Duloxetine on the parotid gland of male albino rats.

(histological and immunohistochemical study)

Amal M. Elsafy Elshazly1, Bodour Baioumy 1., Neama Mahmoud Taha 2, Asmaa Y.A. Hussein 3 and Yasmeen Mohammed Ismail El Sayed 4, and Osama foad 1.
Department of Anatomy and Embryology 1, Department of Forensic Medicine and Clinical Toxicology 3, Department of pharmacology4, Faculty of Medicine, Benha University.
Department of physiology, Umm Al-Qura University, Saudi Arabia 2,
Corresponding author: Amal Elshazly, **Mobile**:(+20)1222924128,**Email:**amal.elshazly79@yahoo.com

https://orcid.org/0000-00031051-7241

ABSTRACT:
Background: Duloxetine is an antidepressant drug utilized for treatment of anxiety disorders and depressive disorders. This study aimed to compare the effect of Rosmarinic acid (RA) on the parotid gland as natural antioxidant with the potential therapeutic effects of mesenchymal stem cells on treating the toxic effect of Duloxetine on the parotid gland. **Material & methods:** 60 male albino rats were classified into 4 groups, 15 rats in each group. The first group (G1):control group receive no treatment., group 2 (G2): received 10 mg/kg/d duloxetine for 12 week, group3 (G3): received Duloxetine the same as (G2) and received at the same time 120 mg/kg/d Rosmarinic acid for 12 week, group4 (G4): received Duloxetine the same as (G2) then single injection of MSCs just after stopping of Duloxetine , In all groups animals were sacrificed after 16 weeks following the beginning of the study. For histological evaluation, the parotid gland was stained with hematoxylin and eosin, and Mallory trichrome stain was used for the demonstration of collagen fibers. Also, Transmission electron microscope and immunohistochemistry using caspas-3 were used to examine the parotid gland. **Results:** Examination of parotid sections in G2 revealed inflammatory cells infiltration and massive distortion and vacuolation of serous cells, however G3 and G4 showed marked improvement in the histological structure of the parotid gland. **Conclusion:** MSCs and RA have good effect in decreasing the toxic effect of Duloxetine administration on the parotid gland with insignificant difference between the two methods.
Keywords: Duloxetine, Rosmarinic acid, MScs ,parotid toxicity.

INTRODUCTION: Depression is one of the most common causes of health retardation, decreased productivity and loss of interest in work. The disease leads to a sever decrease in quality of life for those afflicted and their nearest ones. Mental Disorders' diagnostic and Statistical Manual provides a description of depression's emotional symptoms including the loss of interest, sadness, suicidal attempt, and guiltiness. **(1)**

There are many methods to treat depression and anxiety. Medicines are an alternative, psychotherapy such as cognitive behavioral therapy (CBT) is another. In drug therapy there are many classes of medicines to choose between. The first discovered class of drugs for treatment of depression is tricyclic antidepressants (TCAs). But TCA has many side effects which may lead discontinuation of treatment. These side effects are due to the non-selective binding to various receptors. Also, the overdose may lead to severe arrhythmias. So, TCAs use is restricted. Another

class of antidepressant is introduction of selective serotonin reuptake inhibitors (SSRIs) they are described as being selective due to their major effect on serotonin (5-hidroxitriptamina; 5-HT), not on other neurotransmitters. They are able to mitigate moderate to severe depression symptoms. They are relatively safest and has typical result in less side effects compared to TCAs. Moreover, through increasing serotonin levels in the brain by inhibiting serotonin reuptake, leading to higher availability of serotonin, the SSRIs are able to mitigate depression. However, they can have severe side effects including delayed ejaculation, anorgasmia, and sexual dysfunction and there could be a decrease in libido in about 60% of patients **(2)**, sleep disturbances, anorexia, constipation and dry mouth **(3)**.

A new class of SSRI antidepressants are the drug of choice for the treatment of depression because they are more effective, have fewer side effects, and are well tolerated compared to other antidepressants classes and resulting in more effective control of depression emotional and physical symptoms. This class of antidepressants is used for major depressive disorder (MDD) and possibly for anxiety disorders treatment. According to Cashman and Ghirmai **(4)**, dually has several advantages compared to other antidepressant drugs as it treats a wide range of symptoms. Duloxetine is a part of this class, which was proven in August 2004 **(5)** to treat depression, MDD, neuropathic pain, fibromyalgia **(6)**, generalized anxiety disorder (GAD) **(7)** and diabetic neuropathy. And also, enormous success in chronic musculoskeletal pain treatment, which involves chronic pain of low back and osteoarthritis, has been recently reported by duloxetine **(8)**. There is also a putative relationship between its analgesic efficacy in the center of the brain and its effect on descending inhibitory pain pathways. Duloxetine is also recommended in severe dental and paradental pain. Duloxetine is used as the first-option medication as in some reports in dentistry for burning mouth syndrome (BMS) **(9)**. Duloxetine can significantly mitigate chronic nonorganic oro-facial pain as confirmed by Nagashima et al **(10)**. Its effect of reducing the pain began to appear 2 wks. after starting treatment. Duloxetine effects of pain mitigation have appeared regardless presence or absence of the baseline depressive symptoms. Most prescribed antidepressant medications and the number of significant oral reactions is related, which include dysgeusia, tongue oedema with discoloration, xerostomia, sialoadenitis, glossitis, and stomatitis. These oral reactions appear because of dysfunction of salivary gland. Burning sensation and taste alteration are caused by reduction of saliva production **(11)**.

A range of cell types may be developed from bone marrow-derived stem cells. Immediately after bone marrow-derived mesenchymal cells injection, several reactions are possible including the stem cells homing to the bone marrow and being directed to the injured sites, where they are driven to produce a significant number of growth factors and cytokines. In ischemic areas BM-MSCs may promote vascularization and angiogenesis through their paracrine activities. Consequently, they may initiate the healing process by stimulating the development of endogenous stem cells. **(12)**

Rosmarinic acid (RA) is a natural phenolic chemical which is water-soluble, is one of the S glabra active principal constituents and is extensively diffused in several plant species. Multiple pharmacological effects of RA include anti-inflammatory, antiangiogenic **(13)** and anticancer **(14)**. Its antioxidant function may interfere with unsaturated fatty acids for lipid peroxyl group binding, therefore interfering with the lipid peroxidation chain reaction and slowing it down. RA

inhibits free radical-induced cell damage and has a greater protective effect on the parotid gland than other several natural antioxidants, as chlorogenic acid, folic acid and caffeic acid. RA has a protective effect against the damages caused by ionizing radiation. **(15)**

Subject and method:

Animals:60 male Albino rats with about 200 ± 30 g weight, obtained from Benha University's Faculty of Veterinary Medicine animal house; they were housed at 12 hr light/dark cycle and an appropriate temperature. Prior to the experimental investigation, the animals were kept for 10 days and fed a basic diet.

Drugs:

DULOXETIN: The antidepressant drug duloxetine (Duloxeprin), was purchased from (UTOPIA) medical Company in Egypt in the form of capsules with 30mg /cap concentration. These capsules were evacuated and dissolved in distilled water to a concentration of 10 mg/ml. rats in G 2, G 3 and G4 received 10 mg/kg body weight/daily duloxetine using oro-pharyngeal tube.**(16)**.

ROSMARINIC ACID: Rosmarinic acid (RA) was purchased from (Sigma-Aldrich Chemie Gmbh, Munich, Germany) in the form of water-soluble powder and was given with intragastric tube daily after dissolving it in distilled water in a dose of 120 mg/kg body weight for 12 weeks.**(17)**

Kits: The bio-diagnostic kits were purchased from Diagnostic and Research Reagents (Giza, Egypt) for estimation of Malondialdehyde (MDA) and Glutathione (GSH) levels.

Experimental protocol: 60 male albino rats were equally classified into into 4 groups of 15 rats in each group. G1:control group didn't receive any treatment., G2: received by Oro-pharyngeal tube 10 mg/kg/d Duloxetine dissolved in distilled water for 12 week, G3: received duloxetine the same as group 2 and received at the same time 120 mg/kg body weight RA in the form of powder dissolved in distilled water by intragastric tube for 12 week, G4: received duloxetine the same as group 2 for 12 week and then single injection of (**BMMSCs)** $1x10^6$ cells by intravenous injection at tail vein. In G 2 ,G3 and G4 animals were sacrificed 16 weeks following the beginning of the study.

Histological study: By intraperitoneally anesthetic overdose of ≥0.86 mg/kg sodium pentobarbital, animals were euthanized, then sacrificed by cervical dislocation and their parotid glands were excised, preserved in formalin 10%, and solidified into paraffin blocks. Using a rotary microtome (LEICA RM 2125; UK), these blocks were sliced to a 5 m thickness. Hematoxylin and eosin (H&E), the conventional stain of histological examination were used for staining the blocks, and Mallory (MT), a specialized stain for assessing collagen fibers **(18)**. Using a light microscope (Olympus-Bx; 4500) equipped with a digital camera (Nikon-Coolpix; 4500) and objective lens magnifications of ×200 and ×400, slides were examined and histomorphometric evaluation were performed .

Immunohistochemical analysis:

Using the avidin-biotin peroxidase complex method, then by diaminobenzidine (DAB) staining, Caspase-3immunohistochemical was performed **(19)**. For blood elimination, 10 ml of 0.9% saline

solution was used for cleaning the right parotid which then frozen for biochemical analysis. For the histopathological examination, left parotid gland was prepared.

Biochemical analysis:

Right parotid gland samples were perfused to remove RBCs and clots, homogenized in 0.9% saline solution, centrifuged for 15 min at 3000 rpm, and the supernatant was stored at -20°C until detection of parotid MDA, the breakdown product of lipid peroxidation **(20)**. Commercial kit (Biodiagnostic, Egypt) was used for detection of the amount of glutathione peroxidase (GSH-Px) in the parotid gland **(21)**

Morphometric study:

In 10 randomly chosen microscopic fields at a magnification of X 200 for each specimen, by using image analysis software (Image j. version 1.46), Caspase-3 immune-positive staining and area percent of deposition of collagen fibre was determined

Preparation of BM- MSCs:

Extract of BMMSCs was acquired from the Banha University Histology Department, Faculty of Medicine, Stem Cell Research Unit.

Labeling Of Stem Cells with PKH26 Dye:

PKH26 fluorescent linker dye was uses for labelling the MSCs after isolation during the 4th passage. PKH26 is a red fluorochrome with 567 nm emission and 551 nm excitation. Both proliferative and biological activities are preserved in the labelled cells. Therefore, the linker is suitable for long-term in vivo cell tracking, in vitro cell labelling, and in vitro cell proliferation study. The dye is stable and will proportionally divide as cells divide. Detection of injected cells homing in the rat's tongue: 1wk. after MSCs transplantation into the rat, rat parotid was inspected with a fluorescent microscope to detect the cells dyed with PKH26 dye to confirm the injected cells engraftment into the parotid gland of Gr4, cells tagged with PKH 26 exhibit substantial red autofluorescence. **(Fig.1)**.

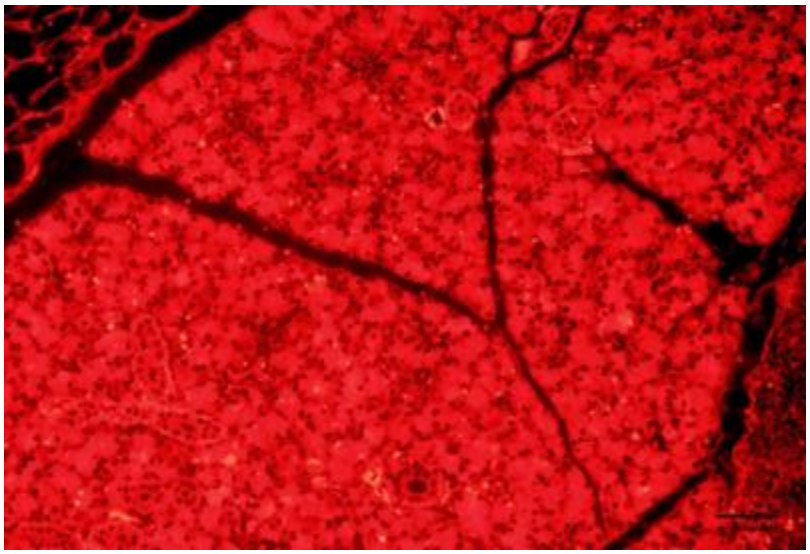

Fig 1: A Photomicrographs of PKH26 fluorescent-stained sections revealing many differentiated red fluorescent BMSC distributed in acinar cells and ducts all over the parotid section (PKH26 ×200)

Electron microscopic studies:

The left parotid glands were extracted and putted rapidly for 4 h in 2.5 % phosphate-buffered glutaraldehyde, and then fixed for 2 h in in 0.1 mol/L 1 % osmium tetroxide. In ascending grades of alcohol, the specimens were dehydrated, to select the suitable sites for ultrathin sections (50-60 nm thick) semithin sections were stained with toluidine blue, then by ultramicrotome they were double stained with lead citrate and 2% uranyl acetate, and then a JEM-1200XXII, Transmission Electron Microscope UK transmission electron microscope at the Faculty of Medicine, Benha University was used for examination and photographing **(22).**

Ethical approval:

This experimental research was evaluated and approved by the Research Ethical Committee of Faculty of Medicine, Benha University ,Rc.14.10.2022.

Statistical analysis:

The data was statistically analyzed using SPSS version 20. One-way analysis and the t-test at a tan significance level $P \leq 0.01$ was used express the data as mean ± SD for all data.

RESULTS

Biochemical analysis (Table 1):

In G 2, the MDA level was significantly higher compared to the control group ($P \leq 0.01$), whereas it was significantly lower in G 3 and G4 compared to G 2 ($P \leq 0.01$).

GSH-Px activity was significantly lower in G 2 compared to the control group ($P \leq 0.01$), but it was significantly higher significantly in G 3 and 4 compared to G 2 ($P \leq 0.01$).

Table (1): Statistical comparisons between mean values of the MDA and the GSH in different studied groups using ANOVA (analysis of variance) test.

groups	MDA (nmol/g tissue) ± SD	GSH (nmol/g tissue) ± SD
Control group	8.03 ± 1.51	23.26± 1.99
Duloxeten group	18.00 ± 0.33**	17.81 ± 1.33**
RA group	9.63 ± 0.51*	22.03 ± 1.64*
MSC group	8.93 ± 0.54 *	22.54 ± 1.11*

The data are shown as the mean ± standard deviation SD (in each group). a Significant difference relative to the control rats, ** significant difference relative to the control group, and *significant difference compared to the Duloxeten group. (MDA: malondialdehyde & GSH: reduced glutathione)

Histological result:

H&E staining:

The parotid sections stained with H&E from G1 revealed nearly normal acini composed of serous cells, striated excretory duct lined by cuboidal epithelium and striated duct lumen can be observed (fig. 1), in G2: parotid sections revealed massive collagen infiltration around ducts , mononuclear inflammatory cells infiltration can be observed in between serous acinar cells with pyknosis of some nuclei of serous cells can be seen, blood vessels were congested , abnormal division in cuboidal epithelium which lined striated excretory duct (fig. 2). Also, we found in same group interlobular connective tissue degeneration and serous cells duct distortion and vacuolation (fig. 3).

While in G3, parotid sections showed small vacuoles in serous cells and focal area of collagen fibers between the serous acini can be observed with slight fibrosis around the ducts and nearly normal serous acinar cells (fig. 4), In G4 parotid sections showed most probably normal architecture of parotid tissue with normal serous acinar cells and normal striated excretory duct and the lumen of excretory duct can be seen, also the excretory duct lined by normal cuboidal epithelium (fig. 5)

Mallory's trichrome stain:

Mallory's T-stained parotid section of rat from G1 revealing no collagen fibers in between the serous acini and minimal collagen fibers around the ducts, but in G2 showed extensive accumulation of collagen fibers in between acinar cells and around ducts. In G3 showed that the ducts were surrounded with a modest number of collagen fibres. Moreover, in G4, showing minimal collagen fibers in between the serous acini and around the ducts. (fig. 6)

Caspase-3 Immuno-histochemical staining:

G1parotid sections showing negative Caspase-3 Immuno-histochemical staining is observed within the serous acini and ducts, and in G2 showing strong positive Caspase-3 Immuno-histochemical staining is observed within the acinar cells and ducts. Moreover, in G3 showing weak Caspase-3 Immuno-histochemical staining can be seen within the acinar cells. While in G4 showing negative Caspase-3 Immuno-histochemical staining is observed within the acinar cells and ducts. (fig. 7)

Morphometric results:

Table 2 and histogram 1 showed the mean area % of deposition of collagen fibers in the sections of parotid gland for all studied groups. The mean area % of caspase-3 expression in parotid gland sections demonstrated in Table 3 & histogram II. G2 demonstrated a significant increase in caspase-3 immuno-positive expression and collagen fibre deposition compared to G1. Compared to G2, caspase-3 immunopositive expression and the % of deposition of collagen fibres decreased significantly in G3 and G4. While there was a non-significant decrease in caspase-3 immuno-positive expression and main area percent of collagen fibre deposition in G4 compared to G3.

Mean % ± SD	Group I	Group II	Group III	Group IV
Mallory %	5.36 ± 1	28.53 ± 4.9	11.45 ± 3.1	6.19 ± 0.95
Significance ≤ 0.05	With group II	With groups I, III & IV	With group II	With group II

Table (2) showing mean values of area percent of Mallory trichrom stain ± SD in the 4 groups

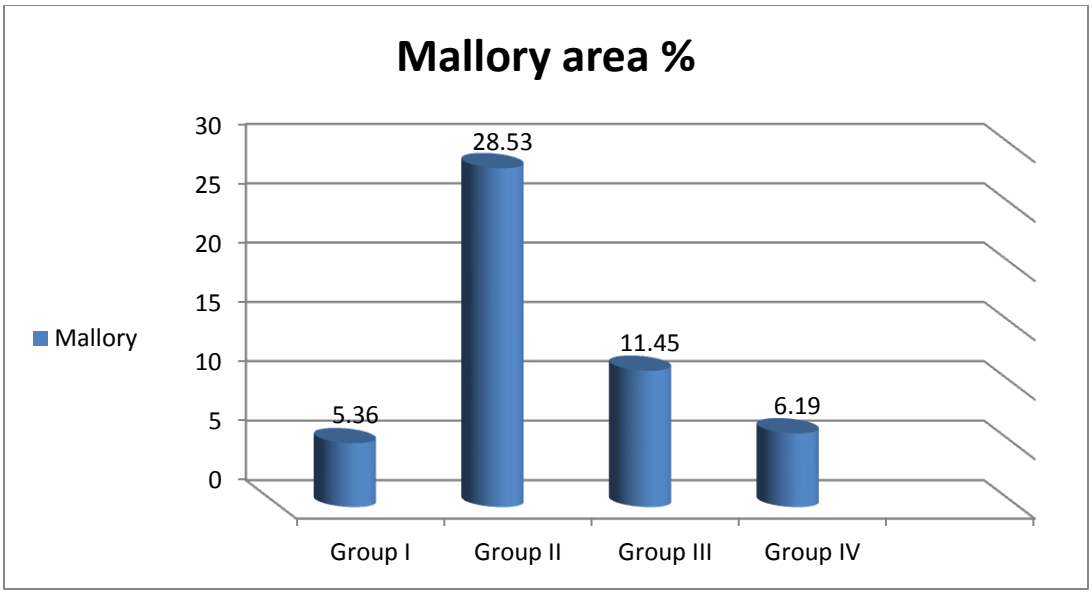

Histogram (I) showing mean values of area percent of Mallory trichrome stain in the four groups.

Mean % ± SD	Group I	Group II	Group III	Group IV
Caspase 3 %	4.3 ± 1.8	36.9 ± 10.8	12.4 ± 1.1	5.28 ± 1.4
Significance ≤ 0.05	With group II	With groups I, III & IV	With group II	With group II

Table (3) showing mean values of area percent of Caspase3 immunoreactivity ± SD in the four groups

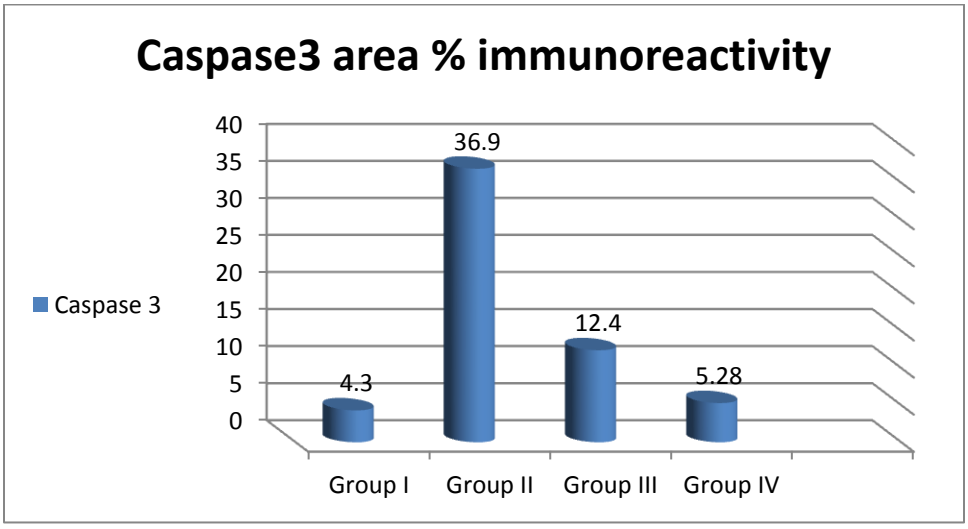

Histogram (II) showing mean values of area percent of Caspase3 Immunoreactivity in the 4 groups.

Electron microscopic results:

Ultrastructure of parotid gland in G1 revealed pyramidal shape acinar cells, their nuclei present at basal side, normal shaped mitochondria, rough endoplasmic reticulum (RER) and the secretory granules show homogeneous high electron dense, with intact junctional complex between the cells can be observed. (fig. 8)

Ultrastructure of parotid gland G2 showed irregular and indentation of nuclei of serous acinar cells, decrease of secretory granules in distorted cells with dilated RER dilated smooth endoplasmic reticulum, less electron dense nucleus, partial lysis of cristae of mitochondria, rarified cytoplasm can be observed. (fig. 9)

Ultrastructure of parotid gland in G3 showing serous acinar cells have mild irregular euchromatic nuclei, swollen degenerated mitochondria, normal RER, and numerous electron dense secretory granules can be notice. (fig. 10).

Ultrastructure of parotid gland G4 showing serous acinar cells. The serous acinar cells have large regular euchromatic nuclei, extensive regular parallel cisternae of RER, nearly normal mitochondria and numerous electron dense secretory granules can be seen. The lateral borders of acinar cells are closely interdigitated, junctional complex is observed between the adjacent cells. (fig. 11)

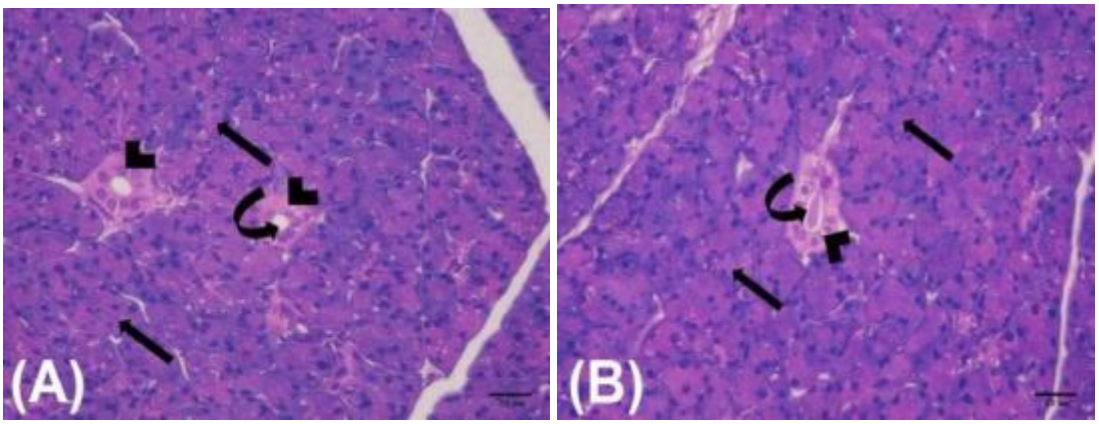

Fig. 2: A photomicrograph of a section in parotid gland of (G1) control group: (A) showing nearly normal acini composed of serous cells (arrow), striated excretory duct lined by cuboidal epithelium (arrowhead) and striated duct lumen (curved arrow) can be observed. (B) showing more or less normal acini composed of serous cells (arrow), striated excretory duct lined by cuboidal epithelium (arrowhead) and striated duct lumen (curved arrow) can be observed (H&E ×400).

Note, interlobular connective tissue can be observed.

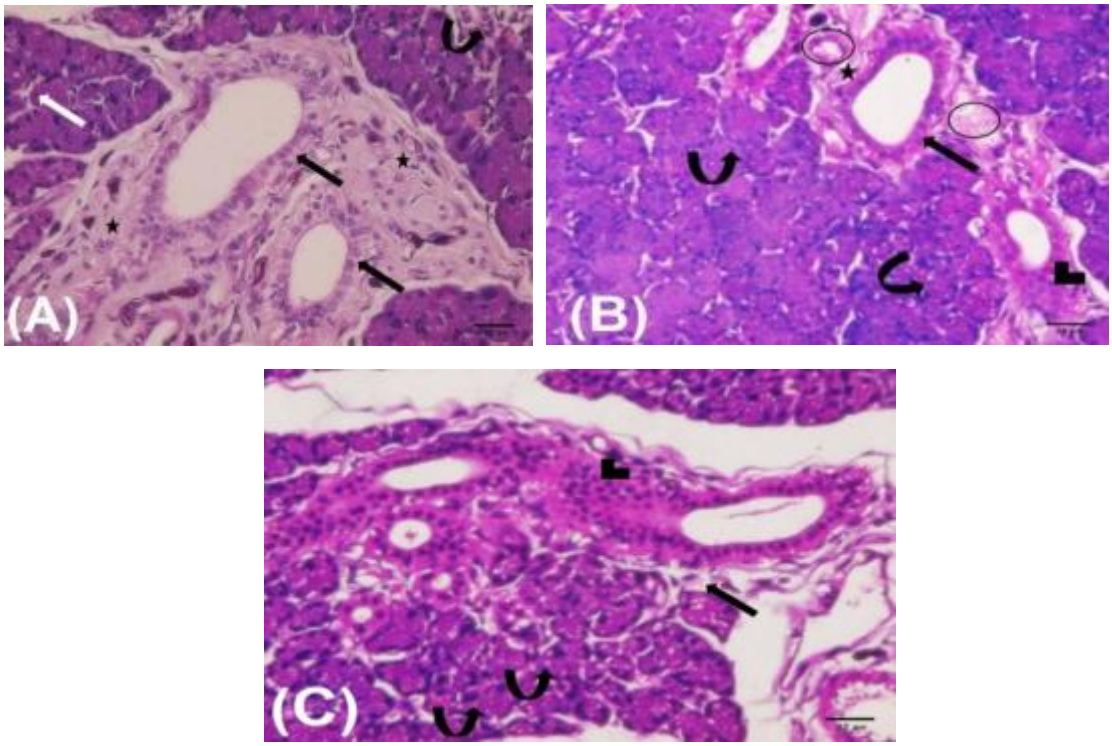

Fig. 3: A photomicrograph of a section in parotid gland of (G2) (duloxetine group) :(A) showing massive infiltration of collagen (astric) around ducts (black arrow), mononuclear inflammatory cells infiltration (curved arrow) can be observed in between serous acinar cells (S). Note, pyknosis of some nucleus of serous cells (white arrow) can be seen. (B) showing infiltration with collagen (astric) around ducts (arrow), blood vessels were congested (circle), abnormal division in cuboidal epithelium which lined striated excretory duct (arrowhead). Note, pyknosis of some nucleus of serous cells (curved arrow) can be seen. (C) showing massive abnormal division in cuboidal epithelium which lined striated excretory duct (arrowhead), degeneration of interlobular connective tissue (arrow), distortion and vacuolation of serous cells (curved arrow). (A, B, C are H&E ×400)

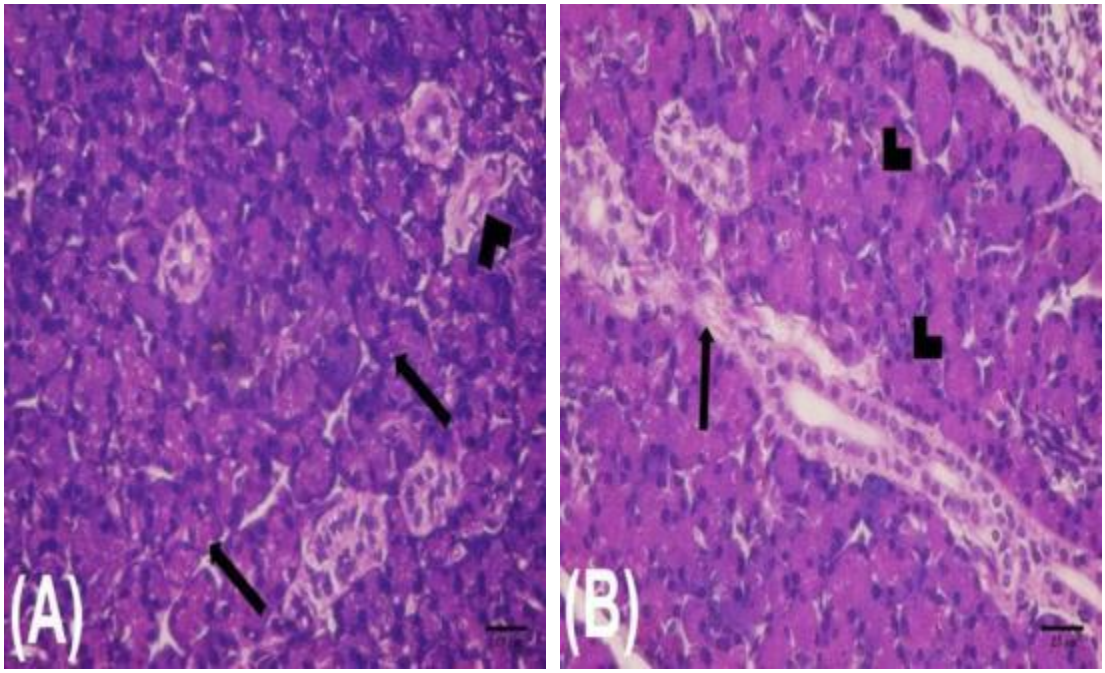

Fig. 4: A photomicrograph of a section in parotid gland of (G3) (Duloxetine +RA) :(A) showing small vacuoles in serous cells (arrow), focal area of collagen fibers (arrowhead) between the serous acini can be observed. (B) showing slightly fibrosis around the ducts (arrow), nearly normal serous acinar cells (arrowhead). (H&E ×400)

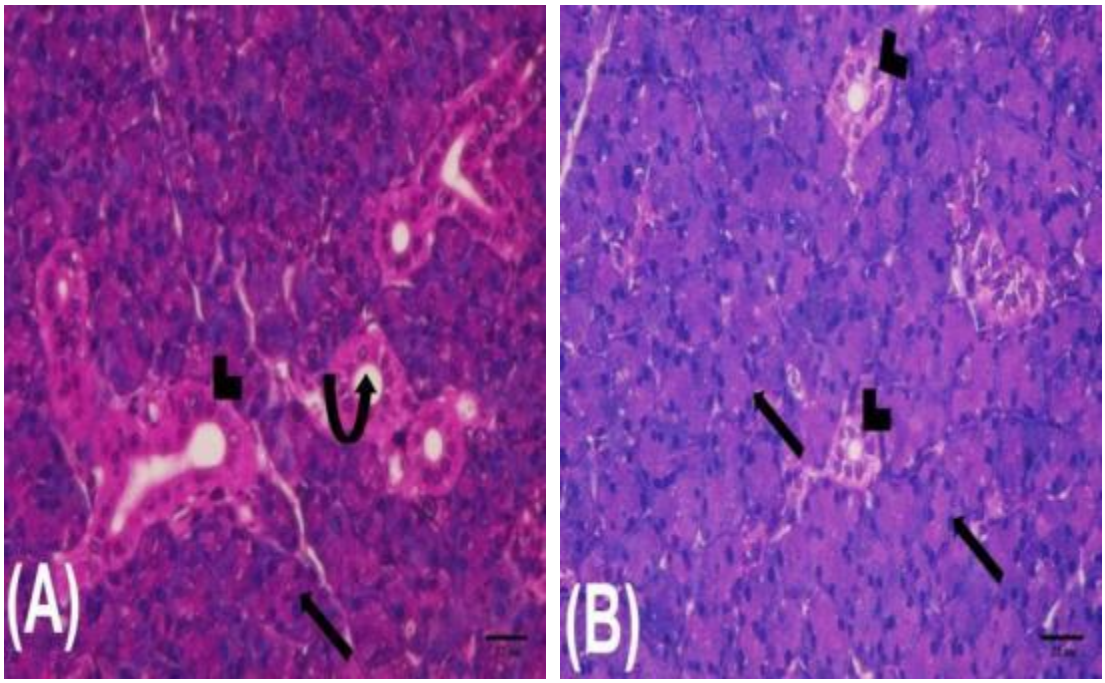

Fig. 5: A photomicrograph of a section in parotid gland of (G4), (duloxetine + MSCs): (A) showing most probably normal architecture of parotid tissue with normal serous acinar cells (arrow) and normal striated excretory duct (arrowhead), lumen of excretory duct (curved arrow) can be seen. (B) showing most probably normal serous acinar cells (arrow) and nearly normal striated excretory duct lined by cuboidal epithelium (arrowhead) can be observed (H&E ×400).

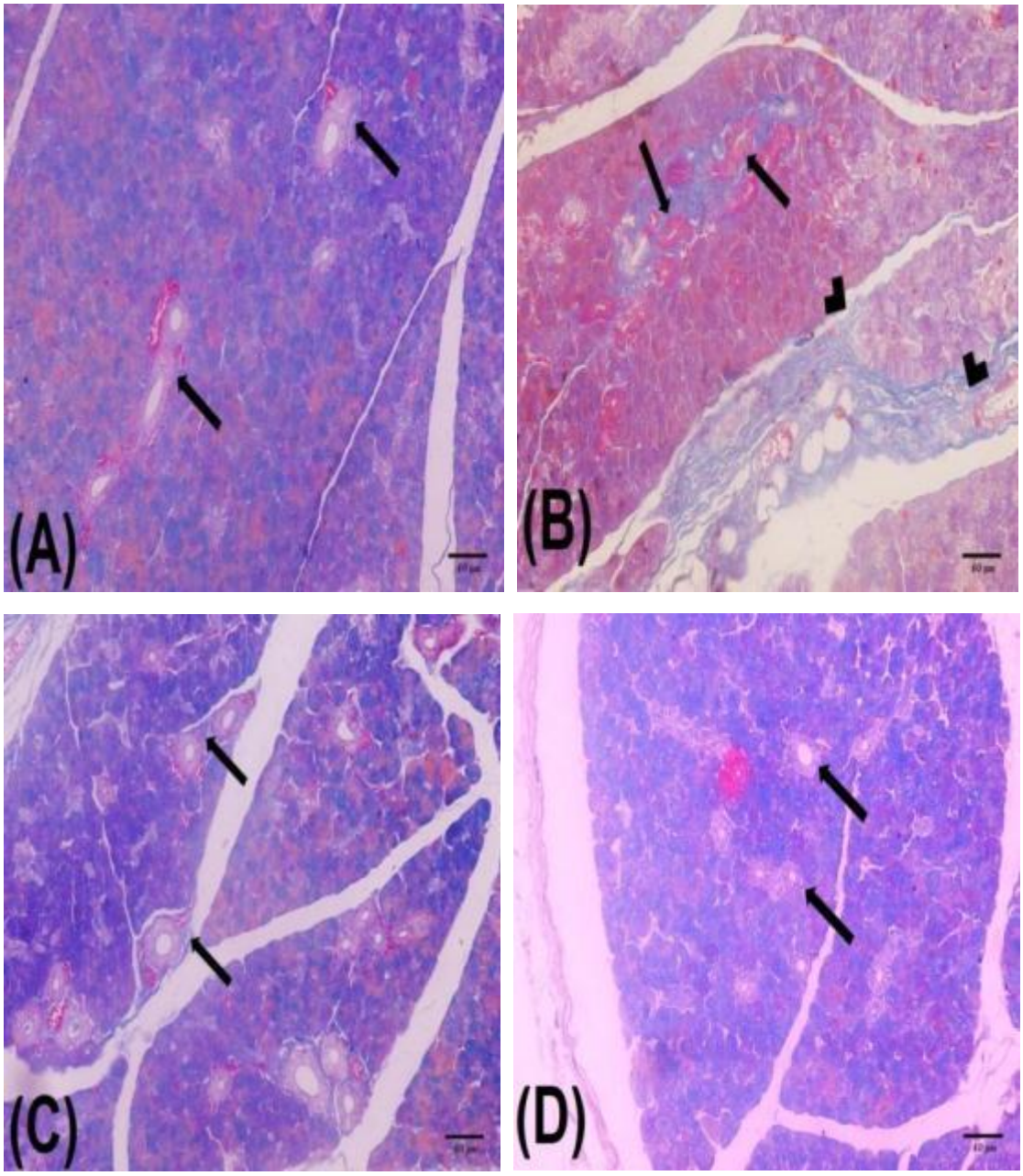

Fig. 6: A Photomicrograph of Mallory's Trichrome stained parotid sections:

(A) section from (G1) control group showing minimal collagen fibers (arrow) around the ducts and no collagen fibers inbetween the serous acini, (B) section from duloxetine group (G2) showing extensive accumulation of collagen fibers (arrow) around ducts and in between acinar cells (arrowhead). (C) section from (G3) (Duloxetine +RA) showing moderate amount of collagen fibers (arrow) around the ducts. And (D) section from group4 (G4), (duloxetine + MSCs) showing minimal collagen fibers (arrow) around the ducts and in between the serous acini. (A, B, C and D are Mallory's Trichrome x 200)

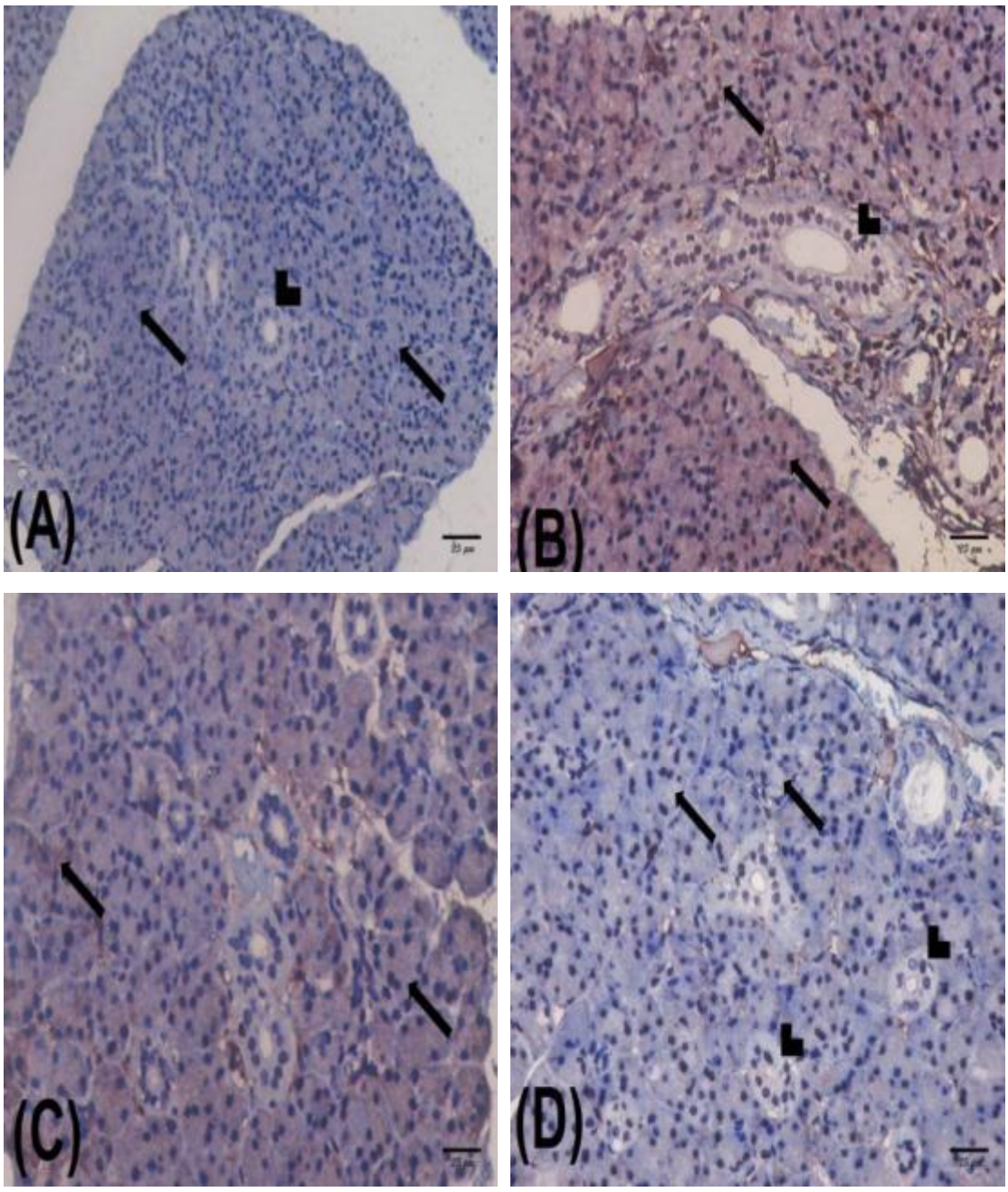

Fig 7: A Photomicrograph of: (A) a section in the parotide of group1(G1) control group showing negative Caspase-3 Immuno-histochemical staining is observed within the serous acini (arrow) and ducts (arrowhead). (B) a section in the parotid of duloxetine group, group2 (G2) rat showing strong positive Caspase-3 Immuno-histochemical staining is observed within the acinar cells (arrow) and ducts (arrowhead). (C) a section in the parotid of group 3(G3) (Duloxetine +RA) rat showing weak Caspase-3 Immuno-histochemical staining can be seen within the acinar cells (arrow). (D) a section in the parotid of group4 (G4), (duloxetine + MSCs) rat showing negative Caspase-3 Immuno-histochemical staining is observed within the acinar cells (arrow) and ducts (arrowhead). (A, B, C and D Caspase-3 x400).

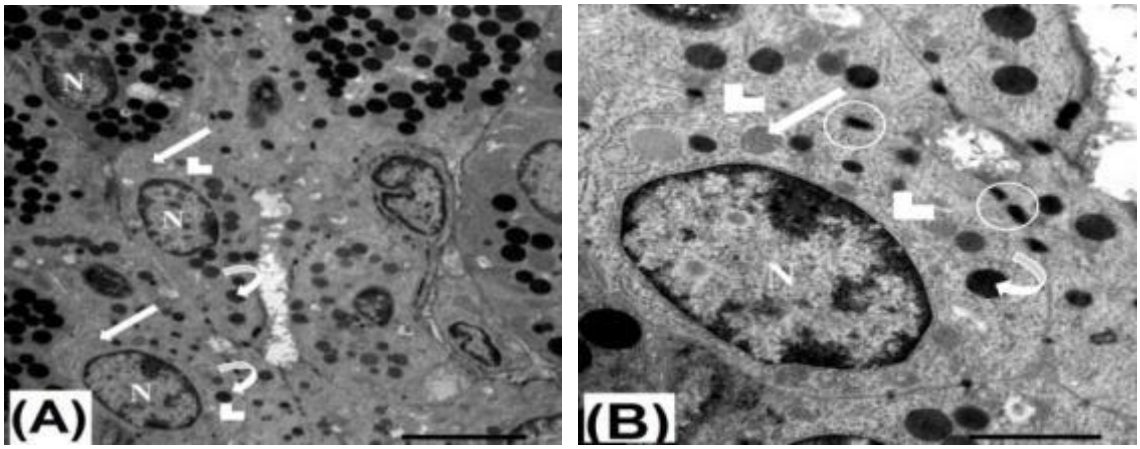

Fig. 8: Ultrastructure of parotid gland in group1(G1) control group: (A) showing pyramidal shape acinar cells, their nuclei exist at basal side (N), mitochondria (arrow), RER (arrowhead). The secretory granules show homogeneous high electron dense (curved arrow). (TEM x 8000). (B) showing nearly normal acinar cell, their nucleus exists at basal side (N), mitochondria (arrow), rough endoplasmic reticulum (arrowhead). The secretory granules show homogeneous high electron dense (curved arrow). Intact junctional complex between the cells can be observed (circle). (TEM x 20000).

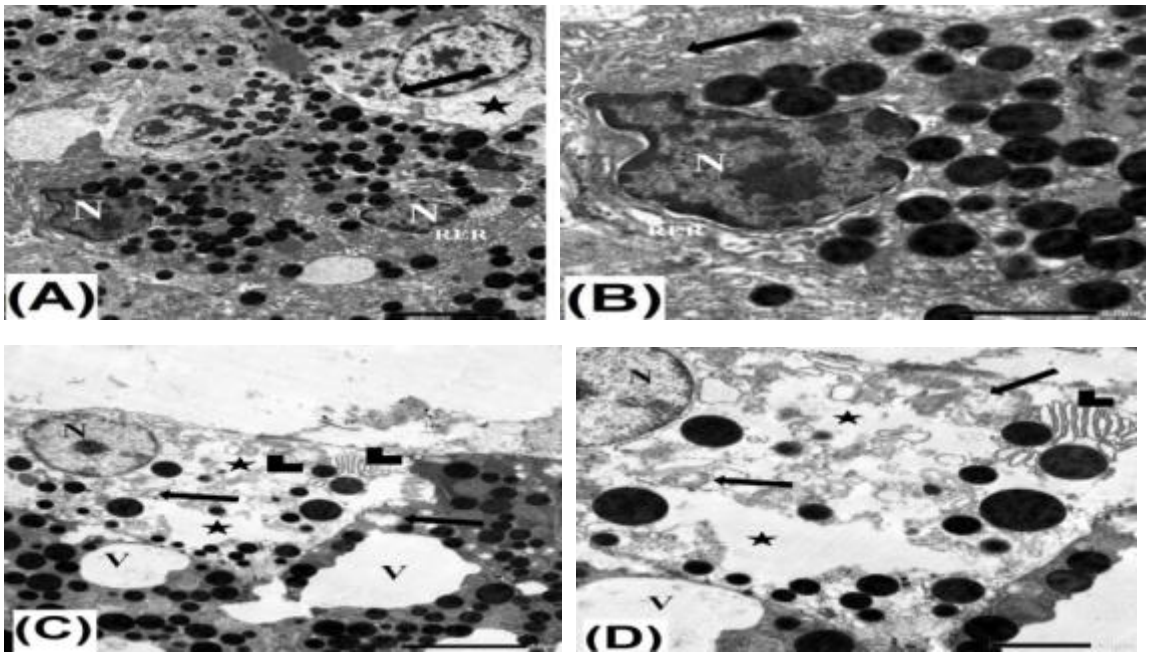

Fig. 9: Ultrastructure of parotid gland in duloxetine group, group2 (G2): (B) showing irregular and indented of nuclei of serous acinar cells with dilated RER, less electron dense nucleus (N), partial lysis of cristae of mitochondria (arrow), rarified cytoplasm (astric) can be observed. (TEM x 8000). (B) showing irregular and indented of nuclei of serous acinar cells with dilated rough endoplasmic reticulum (RER), less electron dense nucleus (N), dilated smooth endoplasmic reticulum (arrow) can be observed. (TEM x 20000). (C) showing distortion of serous acinar cells with dilated and damaged rough endoplasmic reticulum (arrowhead), less electron dense nucleus (N), swollen degenerated mitochondria (arrow), decrease of secretory granules in distorted cell and rarified cytoplasm (astric) can be noticed. Notice, large vacuoles (V) can be observed in serous cells. (TEM x 8000). (D) showing distortion of serous acinar cells with dilated and damaged rough endoplasmic reticulum (arrowhead), less electron dense nucleus (N), swollen degenerated mitochondria (arrow), decrease of secretory granules in distorted cell and rarified cytoplasm (astric) can be noticed. Notice, large vacuoles can be observed in serous cells. (TEM x 20000).

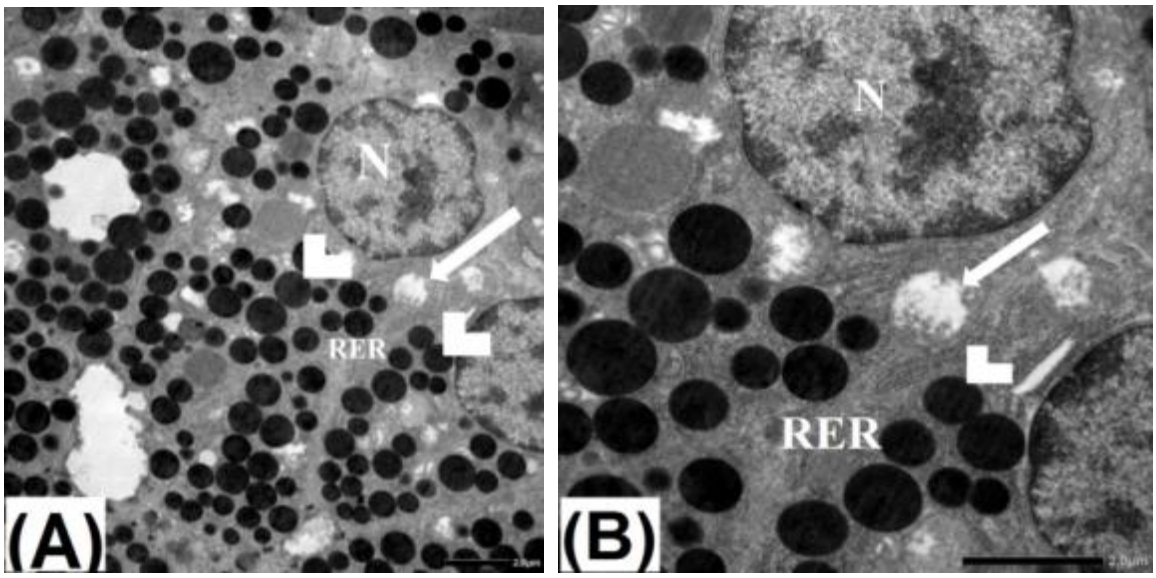

Fig. 10: Ultrastructure of parotid gland in group 3(G3) (Duloxetine +RA): (A) showing serous acinar cells have mild irregular euchromatic nuclei (N), swollen degenerated mitochondria (arrow), normal RER, and numerous electron dense secretory granules (arrowhead) can be noticed. (TEM x 8000). (B) showing serous acinar cells have mild irregular euchromatic nuclei (N), swollen degenerated mitochondria (arrow), normal rough endoplasmic reticulum (RER), and numerous electron dense secretory granules (arrowhead) can be noticed. (TEM x 20000).

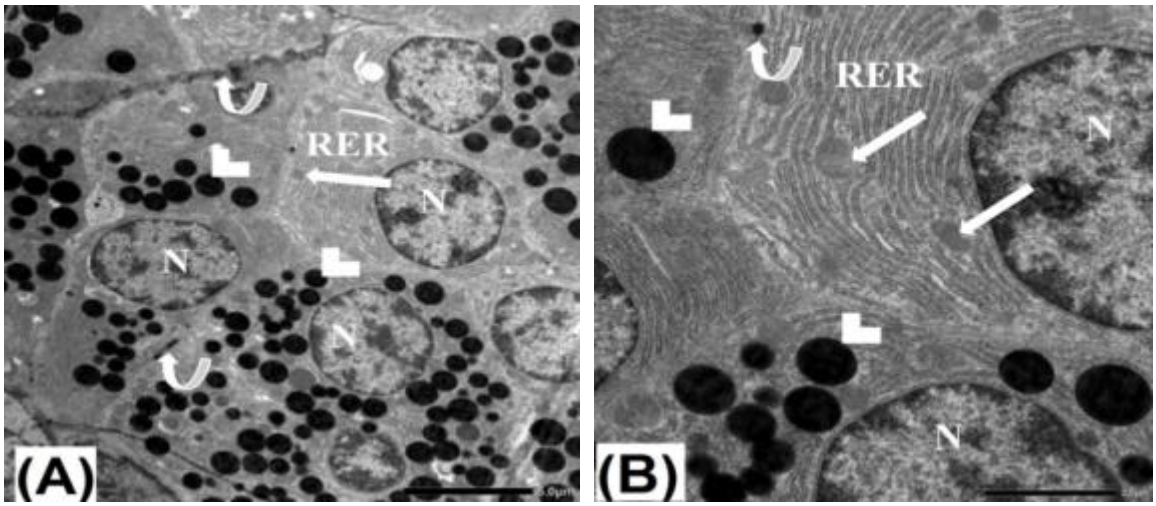

Fig. 11: Ultrastructure of parotid gland in group4 (G4), (duloxetine + MSCs) :(A) showing serous acinar cells. The serous acinar cells have large regular euchromatic nuclei (N), extensive regular parallel cisternae of RER, mitochondria (arrow) and numerous electron dense secretory granules (arrowhead) can be seen. The lateral borders of acinar cells are closely interdigitated, junctional complex is observed between the adjacent cells (curved arrow). (TEM x 8000). (B) showing serous acinar cells. The serous acinar cells have large regular euchromatic nuclei (N), extensive regular parallel cisternae of rough endoplasmic reticulum (RER), mitochondria (arrow) and numerous electron dense secretory granules (arrowhead) can be seen. The lateral borders of acinar cells are closely interdigitated, junctional complex is observed between the adjacent cells (curved arrow). (TEM x 20000).

DISCUSSION:

Many studies have reported that drugs acting on central nervous system (CNS) have pharmacological actions on the salivary glands. The efforts to interpret the xerostomic effects of these medications have been of great scientific value, revealing their physio-pharmacological effects and providing additional benefits to patients receiving these treatments. Described as being SNRI antidepressants, the duloxetine is used in pain, depression, and anxiety treatment. That is why it is one of the most commonly used medications in adults.

The histological results of the current research revealed that long term intake of duloxetine resulted in marked atrophic and degenerative changes in the parotid gland of adult albino rat, Light microscopic examination showed disorganized acini with disappearance of their lumens. Most nuclei of the acinar cells at the peripheral and pyknotic or darkly stained are observed. These acini are widely Separated with connective tissue fibers and hemorrhage, dilated Ducts with retention of secretion are also observed. Our finding in agreement with Mervet et al, (23) who described a similar picture of marked atrophic and degenerative changes in the lingual salivary glands in the adult albino rat.

Mitochondria are the house of power in eukaryotic cells, and they also regulator of cell function by their role in oxidative stress and apoptosis. The results of the current study were consistent with studies done by Youssef (24), Souza et al (25) and Elmorsy et al (26) who demonstrated that fluoxetine has harmful effect on the histological structure of the pancreatic and hepatic cells. They come backed this toxic effect to the mitochondria and stated that mitochondrial damage result in reduction of ATP with successive biosynthesis failure, maintenance of the cytoskeleton, signaling and ion transport, membrane pumps, oxidative stress and induction of apoptosis. Consequently, in our opinion the marked degenerative changes, cystic transformations and collection of stagnant secretions in the acini and ducts of the lingual glands are caused by ATP reduction and depletion of cellular energy used for transport of secretions.

The balanced production of ROS (reactive oxygen species) and its neutralization in healthy humans was achieved by the production of antioxidant defence, which was primarily caused by the defence mechanisms of the cells via the formation of antioxidants and antioxidant enzymes, which provide protection against oxidative damage to cells and tissues. In long term administration of duloxetine there is deviations in the antioxidant controlling process in many body tissues. (27), RA is a known natural antioxidant that protects against duloxetine's harmful side effects.

In the present study we found that RA group had nearly normal serous acinar cells and slightly fibrosis around the ducts, this was in agreement with Tingting et al, (28) who found that RA reduced the radiation induced toxic damage on the parotid gland of adult albino rat, and resulted in a marked decrease acinar atrophy, less luminal dilation, less vacuolization, increase in acinar number, less interstitial fibrosis, and decrease capillary congestion. The glandular lobule structure got close to be normal.

A substantial number of cytoplasmic vacuoles with shrunken nuclei and loss of acinar outlines were found in the parotid salivary glands in the current study as a result of Duloxetine therapy.

After I.V injection of BMSCs, the parotid gland showed a more regular glandular architecture, In accordance with the findings of Khalili et al., Stem cells have anti-inflammatory and immunostimulatory properties, according to their research on the treatment of NOD (non-obese diabetic) mice with Sjogren's-like disease employing multipotent MSCs as a therapy for autoimmune diseases. (29) BMSCs can be collected by a needle aspiration and divided into a large number of multipotent MSCs. Numerous studies were undertaken to examine the MSCs efficacy as a novel treatment for autoimmune diseases, as rheumatoid arthritis, systemic lupus erythematosus and type 1 diabetes (30).

The Current explanations demonstrated an appropriate homeostatic non-inflammatory translocation of BMSCs into the parotid glands, hence reducing parotid gland morphological alterations. This experimental transfer occurred rather quickly and was observable within the 1st week. MSCs recruited from bone marrow appeared to be primarily responsible for the improved performance of salivary gland tissues via cytokine-mediated interactions with tissue stem cells (31)

Conclusion:

BMSCs were an effective therapy for harmful effects of Duloxetine on salivary glands. Significant non-inflammatory and homeostatic MSCs migration from the bone marrow to the salivary glands increases saliva output and maintains glandular architecture.

In contrast, the current study reveals that the duloxetine-induced increase in ROS generation plays a crucial role in the rat parotid glands pathophysiology. ROS was greatly reduced by RA's direct antioxidative action. Moreover, RA reduced cell apoptosis and suppressed fibrosis in the parotid glands. Therefore, RA has a greater potential for parotid gland injuries treatment than BMSCs, although not to the same degree.

Conflicts of Interest: The authors declare no conflict interest.

Referances:

1. **Fountolakis K, O'Hara R, Apostolosacovides C, *et al* (2003):** Unipolar late onset depression, A comprehensive review. Ann.Gen. Hos. Psych., 2:11- 14.
2. **Clayton A, Pradko A, Croft H, *et al* (2002):** Prevalence of sexual dysfunction among newer antidepressants. J Clin Psychiatry, 63:357–366.
3. **Richelson, E. (2003):** Interaction of antidepressants with neurotransmitter transporters and receptors and their clinical relevance. J Clin Psychiatry, 64: 5–13.
4. **Cashman, J, and Ghirmai S, (2009):** Inhibition of serotonin and norepinephrine reuptake and inhibition of phosphodiesterase by multi-target inhibitors as potential agents for depression. Bioorganic & Medicinal Chemistry, 17: 6890–7.
5. **Iyengar S, Webster A, Hemric S, *et al* (2004):** Efficacy of duloxetine, a potent and balanced serotonin-norepinephrine reuptake inhibitor in persistent pain models in rats. J. Pharmacol. Exp. Ther., 311: 576–84.

6. **Russell J, Mease P, Smith T, *et al* (2008):** Efficacy and safety of duloxetine for treatment of fibromyalgia in patients with or without major depressive disorder: results from a 6- month, randomized, double-blind, placebo-controlled, fixed-dose trial. Pain, 136: 432–444.
7. **Wernicke J, Pritchett Y, Souza D, *et al* (2006):** A randomized controlled trial of duloxetine in diabetic peripheral neuropathic pain. Neurology, 67: 1411–1420.
8. **Skljarevski V, Zhang S, Desaiah D, *et al* (2010):** Duloxetine versus placebo in patients with chronic low back pain: a 12-week, fixed-dose, randomized, double-blind trial. J Pain, 11:1282-90.
9. **Yeon-Dong K, Ji-Hye L, and Jee-Hoon S, *et al* (2010):** Duloxetine in the treatment of burning mouth syndrome refractory to conventional treatment: A case report. Journal of International Medical Research, 42: 879–883.
10. **Nagashima W, Kimura H, Ito M, *et al* (2012):** Effectiveness of duloxetine for the treatment of chronic nonorganic orofacial pain. Clin Neuropharmacol, 35: 273–277.
11. **Nerella N, Mamatha G, and Rajeshwari G, *et al* (2014):** Modified schirmer test–A screening tool for xerostomia among subjects on antidepressants. archives of oral biology, 59: 829– 834.
12. **Nakano-Doi A, Nakagomi T, Fujikawa M, *et al* (2010):** Bone marrow mononuclear cells promote proliferation of endogenous neural stem cells through vascular niches after cerebral infarction. Stem Cell, 28:1292–1302.
13. **Jiang K, Ma X, Guo S, *et al* (2018):** Anti-inflammatory effects of rosmarinic acid in lipopolysaccharide-induced mastitis in mice. Inflammation, 41(2):437-448.
14. **Gonz´alez-Vallinas M, Reglero G, Ram´ırez de Molina A, *et al* (2015):** Rosemary (Rosmarinus officinalis L.) extract as a potential complementary agent in anticancer therapy. Nut Can, 67(8):1223-1231.
15. **Xu W, Yang F, Zhang Y, *et al* (2016):** Protective effects of rosmarinic acid against radiation-induced damage to the hematopoietic system in mice. J Radiat Res.,57 (4) :356-362.
16. **Patel S, Kale P, Addepalli V, *et al* (2015):** Effect of a combination of duloxetine with hydroxyzine on experimental models of anxiety in mice. Indian J. Pharmacol., 47: 173-176.
17. **Sotnikova R, Okruhlicova L, Vlkovicova J, *et al* (2013):** Rosmarinic acid administration attenuates diabetes-induced vascular dysfunction of the rat aorta. J Pharm Pharmacol., 65(5):713-723.
18. **Bancroft JD and Layton C (2013)**: The hematoxylin and eosin. In: Suvarna SK, Layton C, Bancroft JD (eds) Theory practice of histological techniques. Churchill Livingstone, Philadelphia, p:179–220.
19. **Jackson P and Blythe D (2013):** Theoryand Practice of Histological Techniques.7 th ed., Churchill Livingstone of El Sevier. Philadelphia,p:381 - 434.
20. **Ohkawa H, Ohishi N ,Yagi K, *et al* (1979):** Assay for lipid peroxides in animal tissues by thiobarbituric acid reaction. Analytical Biochemistry, 95:351– 358.

21. **Beutler E, Duron O , Kelly M, *et al* (1963):** Improved methods for determination of blood glutathione. J. Lab. Clin Med., 61:882–888.
22. **Wu F, Jin W, Feng J, *et al* (2010):** Propamidine decrease mitochondrial complex III activity of Botrytis cinerea. BMB Rep 43: 614-621.
23. **Mervat M. Youssef, Ahmed M. et al. (2020):** Apoptotic effect of long term administration of antidepressant duloxetine on tongue of albino rat, histological and immunohistochmical study, EDJ., 66: 213:223.
24. **Youssef S. (2017):** Effect of Fluoxetine on the Pancreas of Adult Male Albino Rats and the Possible Protective Role of Omega-3: Light and Electron Microscopic Study. International Journal of Clinical and Developmental Anatomy, 3: 45-56
25. **Souza M, Polizello A, Uyemura S, *et al* (1994):** Effect of fluoxetine on Rat liver mitochondria. Biochemical Pharmacology , 48:535–541,
26. **Elmorsy E, Al-Ghafari A, Helaly A, *et al* (2017):** Editor's highlight therapeutic concentrations of antidepressants inhibit pancreatic betacell function via mitochondrial complex inhibition. Toxicol. Sci., 158: 286-301.
27. **Townsend D, Tew K, Tapiero H, *et al* (2003):** The importance of glutathione in human disease. Biomed Pharmacother, 57:145–155.
28. **Tingting Z, Chang L, Shanshan M, *et al* (2020):** Protective Effect and Mechanism of Action of Rosmarinic Acid on Radiation-Induced Parotid Gland Injury in Rats, journal of Potential Biomarkers of Radiation Damage,1-11.
29. **Khalili S, Liu Y, Kornete M, *et al* (2012)**: Mesenchymal stromal cells improve salivary function and reduce lymphocytic infiltrates in mice with Sjö gren's-like disease. PloS One, 7(6): 38615.
30. **Fotino C, Ricordi C, Lauriola V, *et al* (2010):** A. Bone marrow-derived stem cell transplantation for the treatment of insulin-dependent diabetes. Rev Diabetic Stud.,7(2):144–159.
31. **Lombaert I, Wierenga P, Kok T, *et al* (2006):** Mobilization of bone marrow stem cells by granulocyte colony-stimulating factor ameliorates radiation-induced damage to salivary glands. Clin Cancer Res.,12(6):1804–1812.